Proceedings of the 9ICEG
9th International Congress on Environmental Geotechnics
25-28 June, 2023 | Chania, Greece
© Authors: All rights reserved, 2023
https://doi.org/10.53243/ICEG2023-63

Theoretical Analysis and Numerical Simulation of Hydrothermal Coupled Process in Unsaturated Soils

Y. Wu[1], Z. Chen[1], Y. Wang[1], L. Hu[1*], and Z. Yin[2]

[1]*State Key Laboratory of Hydro-Science and Engineering, Department of Hydraulic Engineering, Tsinghua University, Beijing, China;*

[2]*Department of Civil and Environmental Engineering, The Hong Kong Polytechnic University, Hong Kong;*

[*]*Corresponding author, email: gehu@tsinghua.edu.cn*

ABSTRACT

The vapor in unsaturated soil migrates and condenses due to the temperature gradient, which leads to the change in local water content and further causes engineering problems such as road mud squeezing and frost heave in cold regions. Consequently, the coupled process of water-vapor and heat transfer in soils is one of the major concerns in the study of soil behaviors. This paper establishes the governing equations of water-vapor and heat migration respectively, based on the theoretical framework of mass and energy conservation. Subsequently, a one-dimensional finite element model (FEM) is developed to simulate the hydrothermal coupled process in unsaturated soils such as sand, loam, and clay. The simulation results indicate that water and vapor migrate from the cold end to the warm end under the temperature gradient. The vapor migration is most dominant in sand, followed by loam, and weakest in clay. However, due to the poor water holding capacity, water in sand is significantly affected by gravity, causing the increase of surface water content not noticeable. The simulation results under different initial water content reveal that the vapor migration cannot be ignored when the initial water content is extremely low, and the water migration under the temperature gradient needs to be adequately considered.

Keywords: Hydrothermal coupled process; Unsaturated soil; Finite element model (FEM); Soil type

1 INTRODUCTION

The movements of fluids phases and heat in soils are highly coupled under non-isothermal conditions, which poses a challenge to assess. The evolution of both liquid and gas phases is affected by the temperature gradient and hydraulic gradient, which changes the heat distribution in turn. Many engineering problems in cold and arid regions are associated with this process such as pavement cracking, road mud squeezing, and frost heave (Li et al., 2021). Besides, the water-vapor migration may be accompanied by the movement of salt, resulting in soil salinization. Furthermore, evaporation of water and condensation of vapor at the surface can affect the water and energy balance of the near-surface environment. Therefore, understanding the hydrothermal coupled process is of great significance for engineering constructions, agronomy, and hydrology (Saito et al., 2006).

Up to now, many numerical models have been proposed to simulate the hydrothermal coupled process. In previous models, the vapor migration was supposed to have little effect on the overall water transfer and was ignored. However, experimental results revealed that the vapor can accumulate underneath a cover in unsaturated soils, resulting in a noticeable increase in water content (Zhang et al., 2016). Therefore, vapor migration should be included in the models. The first numerical model considering the water-vapor migration under non-isothermal conditions is established by Philip and De Vries (1957) and De Vries (1958). After that, some researchers further improved the model. Saito et al. (2006) proposed a complete model to study the coupled process in the vadose zone, which was widely used ever since. However, in the model of Philip and De Vries (1957), water in liquid and gas phases are in equilibrium, which is not in line with reality. So, the nonequilibrium coupling model considering a phase change rate was further developed (Smits et al., 2011) and matched well with the experimental data.

Most numerical studies focus on analyzing the influence of external conditions on the hydrothermal coupled process, such as time-varying boundary conditions, and the closed boundary condition. However, internal conditions (e.g., soil type) also play an important role in this process. The hydraulic conductivity, thermal conductivity, and water retention capacity vary with different types of soils (Côté & Konrad, 2005), all of which are closely related to water content (Orakoglu Firat, 2021). Higher hydraulic conductivity means more water-vapor migration, and higher thermal conductivity means faster heat transfer and a shorter time to reach energy equilibrium. As for the water retention capacity, it relates to the water content and reflects the magnitude of the water potential in soils. The lower the water potential is, the more bound it is and the harder it is to migrate. Generally, clay has the lowest water potential at the same water content, i.e., the strongest water retention capacity, compared to sand and silt. All of them affect the coupled migration process of water, vapor, and heat. Therefore, it is necessary to investigate the effect of soil type and water content on the hydrothermal coupled migration process. Song et al. (2017) suggested that vapor condensation in silt is more intense than in sand and clay based on the numerical simulation results. However, the initial water content of the whole soil column in the most numerical study including Song et al. (2017) is the same, which may be inconsistent with the actual spatial distribution of water in the soil due to gravity and needs to be improved.

The main objective of this paper is to make an in-depth analysis of the coupled transfer of water, vapor, and heat in unsaturated soils. We first theoretically derived the governing equations of the hydraulic and thermal fields and established the hydrothermal coupled model. Then we simulated the 1-dimensional hydrothermal coupled migration process in different types of unsaturated soils. At last, the effect of initial water content was further discussed to understand the hydrothermal coupled process in unsaturated soils.

2 MODEL CONSTRUCTION

The governing equations of water-vapor and heat transfer in unsaturated soils are derived respectively in this section, considering a one-dimensional transfer process. Assume a soil element with side lengths of dx, dy and dz, and flow in the z-direction.

2.1 Governing equation of water-vapor transfer

Based on mass conservation, i.e., the increment of water per unit time is equal to the net inflow, the governing equation of water-vapor transfer is built as follows:

$$\frac{\partial(\rho_{\mathrm{l}}\theta_{\mathrm{l}}+\rho_{\mathrm{v}}\theta_{\mathrm{v}})}{\partial t}\mathrm{d}x\mathrm{d}y\mathrm{d}z\mathrm{d}t=\left(-\frac{\partial(\rho_{\mathrm{v}}q_{\mathrm{v}})}{\partial z}-\frac{\partial(\rho_{\mathrm{l}}q_{\mathrm{l}})}{\partial z}\right)\mathrm{d}x\mathrm{d}y\mathrm{d}z\mathrm{d}t \tag{1}$$

$$\frac{\partial(\theta_{\mathrm{l}}+\theta_{\mathrm{ve}})}{\partial t}=-\nabla(q_{\mathrm{l}}+q_{\mathrm{ve}}) \tag{2}$$

where θ is the volumetric content, m^3/m^3; q is the volumetric flux, m^3/m^2/s; ρ is the density, kg/m^3; herein and hereafter, the subscripts l and v denote the water and vapor, respectively; θ_{ve} is the equivalent vapor content, and $\theta_{\mathrm{ve}}=\rho_{\mathrm{v}}\theta_{\mathrm{v}}/\rho_{\mathrm{l}}=\rho_{\mathrm{v}}(\theta_{\mathrm{s}}-\theta_{\mathrm{l}})/\rho_{\mathrm{l}}$, m^3/m^3; θ_{s} is the saturated water content, m^3/m^3; q_{ve} is the equivalent volumetric flux of vapor, and $q_{\mathrm{ve}}=\rho_{\mathrm{v}}q_{\mathrm{v}}/\rho_{\mathrm{l}}$,m^3/m^2/s; $\nabla=\partial/\partial z$.

Previous research has proposed that the water flux is due to hydraulic gradient, temperature gradient, and gravity and the vapor flux is due to hydraulic and temperature gradients (Philip & De Vries, 1957), expressed as follows:

$$q_{\mathrm{l}}=-K_{\mathrm{lh}}(\nabla h+1)-K_{\mathrm{lT}}\nabla T \tag{3}$$

$$q_{\mathrm{ve}}=-K_{\mathrm{vh}}\nabla h-K_{\mathrm{vT}}\nabla T \tag{4}$$

where h (m) is the water head that is negative for unsaturated soils and is related to water content by the soil-water characteristic curve (SWCC); T is the soil temperature, K; K_{lh} (m/s) and K_{lT} (m^2/K/s) are

the isothermal and thermal hydraulic conductivity for water; K_{vh} (m/s) and K_{vT} (m^2/K/s) are the isothermal and thermal hydraulic conductivity for vapor. SWCC model used in this paper is the VG model (van Genuchten, 1980), expressed as

$$Se = \left[1 + \left(-ah\right)^n\right]^{-m} \tag{5}$$

where Se is the effective saturation and, $Se=(\theta_l-\theta_r)/(\theta_s-\theta_r)$; θ_r is the residual water content, m^3/m^3; a (1/m), n, m are fitted parameters.

2.2 Governing equation of heat transfer

The ways of heat transfer include conduction, convection, and radiation. Heat radiation is ignored in this paper. Heat conduction follows Fourier's law, which is expressed as

$$\Phi_{cd} = -\lambda \frac{\partial T}{\partial z} \tag{6}$$

where λ is the thermal conductivity of the soil, W/m/K; Φ_{cd} is the heat flux caused by heat conduction, W/m^2. Thus, for the soil element, the net incoming heat through heat conduction per unit time is

$$\Delta\phi_{cd} = -\frac{\partial \Phi_{cd}}{\partial z}\mathrm{d}x\mathrm{d}y\mathrm{d}z = \nabla\left(\lambda \nabla T\right)\mathrm{d}x\mathrm{d}y\mathrm{d}z \tag{7}$$

Similarly, the net heat inflow caused by heat convection per unit time is

$$\Delta\phi_{cv} = -(C_l \frac{\partial (q_l T)}{\partial z} + C_v \rho_l \frac{\partial (q_{ve} T)}{\partial z})\mathrm{d}x\mathrm{d}y\mathrm{d}z \tag{8}$$

where C_l is the isobaric volumetric specific heat capacity of water, J/m^3/K; C_v is the isobaric mass specific heat capacity of vapor, J/kg/K.

The total heat of the soil element is

$$S = (C_n \theta_n T + C_l \theta_l T + C_v \rho_l \theta_{ve} T)\mathrm{d}x\mathrm{d}y\mathrm{d}z \tag{9}$$

where C_n is the isobaric volumetric specific heat capacity of soil particles, J/m^3/K; θ_n is the volume content of soil particles, m^3/m^3.

So, according to energy conservation and regarding the water-vapor phase transition as an energy sink (marked as Q), the governing equation of heat transfer is derived:

$$\frac{\partial S}{\partial t} = \Delta\phi_{cd} + \Delta\phi_{cv} - Q \tag{10}$$

$$C_p \frac{\partial T}{\partial t} + L_0 \frac{\partial \theta_{ve}}{\partial t} = \frac{\partial}{\partial z}\left(\lambda \frac{\partial T}{\partial z}\right) - C_l q_l \frac{\partial T}{\partial z} - C_v \rho_l q_{ve} \frac{\partial T}{\partial z} - L_0 \frac{\partial q_{ve}}{\partial z} \tag{11}$$

where L_0 is the latent heat of water vaporization, J/m^3; C_p is the isobaric volumetric specific heat capacity of soil, J/m^3/K.

2.3 Model implementation

The coupling model can be established according to Equations 2 and 11. The independent variables are θ_l and T. Detailed expressions of model parameters and related physical quantities used for numerical simulation are summarized in Table 1.

Table 1. *Model parameter expressions and related physical quantities (Saito et al., 2006).*

Parameter	Expression or Value	Unit
Isothermal hydraulic conductivity for water, K_{lh}	$K_{lh}=K_s Se^{l}(1-(1-Se^{1/m})^{m})^2$	m/s
Thermal hydraulic conductivity for water, K_{lT}	$K_{lT}=K_{lh}hG_{wT}/\gamma_0(d\gamma/dT)$	$m^2/K/s$
Isothermal hydraulic conductivity for vapor, K_{vh}	$K_{vh}=D\rho_{vs}MgH_r/(\rho_l RT)$	m/s
Thermal hydraulic conductivity for vapor, K_{vT}	$K_{vT}=D\eta H_r(d\rho_{vs}/dT)/\rho_l$	$m^2/K/s$
The surface tension of water, γ	$\gamma=75.6-0.1425(T-273.15)-2.38\times10^{-4}T^2$	mN/m
Vapor diffusivity in soil, D	$D=2.12\times10^{-5}(T/273.15)^2\theta_v^{10/3}/\theta_s^2$	m^2/s
Saturated vapor density, ρ_{vs}	$\rho_{vs}=\exp(31.37-6016.79T^{-1}-7.92\times10^{-3}T)\times10^{-3}T^{-1}$	kg/m^3
Vapor density, ρ_v	$\rho_{vs}H_r$	kg/m^3
Relative humidity, H_r	$H_r=\exp(hMg/RT)$	1
Enhancement factor, η	$\eta=9.5+3\theta_l/\theta_s-8.5\exp(-((1+2.6/f_c^{0.5})\theta_l/\theta_s)^4)$	1
Mass fraction of the clay, f_c	\	1
Specific heat capacity of soil, C_p	$C_p=C_n\theta_n+C_l\theta_l+C_v\rho_l\theta_{ve}$	$J/m^3/K$
Specific heat capacity of soil particle, C_n	1.92×10^6	$J/m^3/K$
Specific heat capacity of water, C_l	4.18×10^6	$J/m^3/K$
Specific heat capacity of vapor, C_v	1.86×10^3	J/kg/K
Thermal conductivity of the soil, λ	$\lambda=b_1+b_2\theta_l+b_3\theta_l^{0.5}$	W/m/K
Empirical regression parameters, b_1, b_2, b_3	\	W/m/K
Latent heat of water evaporation, L_0	$L_0=\rho_l(2.501\times10^6-2369.2(T-273.15))$	J/m^3
Water density, ρ_l	1000	kg/m^3
Saturated hydraulic conductivity, K_s	\	m/s
Fitting parameter, l	0.5	1
Gain factor, G_{wT}	7	1
The surface tension of water at 25 °C, γ_0	71.89	mN/m
The molecular weight of water, M	0.018	kg/mol
Gravitational acceleration, g	9.81	m/s^2
Universal gas constant, R	8.341	J/mol/K

The COMSOL Multiphysics software is employed to solve the equations and the coefficient partial differential equations (PDEs) interface is used in this paper. We build a one-dimensional model, 3 meters high soil column, as shown in Figure 1a. For the hydraulic field, the upper boundary is zero flux and the lower boundary is given effective saturation. The initial condition is the stationary water distribution without a temperature gradient. Then the upper boundary temperature is set to 278.15K to form a temperature gradient. To cover a wide variety of soils, we select three types of soil to analyze, namely sand, loam and clay. Their physical properties are listed in Table 2, and the soil-water characteristic curves are shown in Figure 1b.

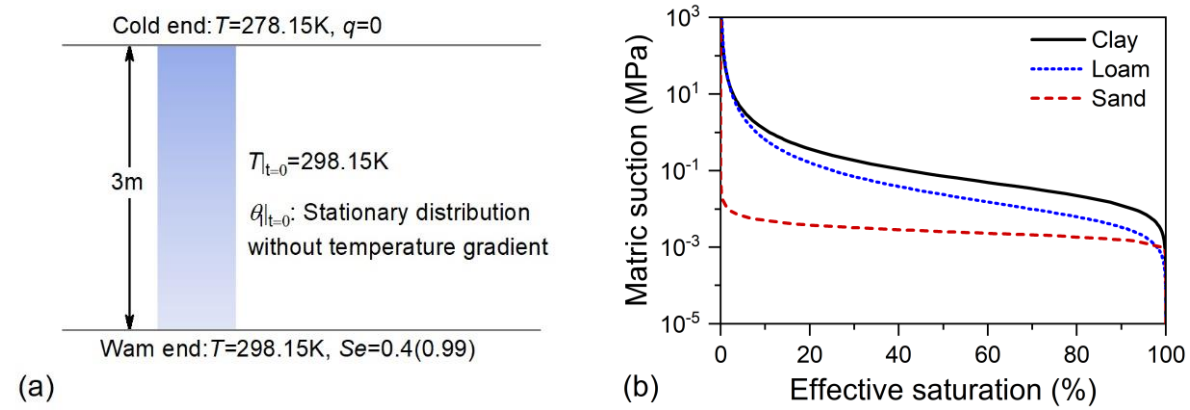


Figure 1. *Diagram of model and soil sample characteristics. (a) Schematic diagram of the numerical model with initial and boundary conditions.(b) Soil-water characteristic curves of selected soil samples.*

Table 2. *Physical properties of selected soil samples.*

Physical Property	Sand	Loam	Clay	Unit
Saturated water content, θ_s	0.43	0.48	0.45	m^3/m^3
Residual water content, θ_r	0.03	0.01	0.15	m^3/m^3
VG parameter, a	4.92	1.55	0.393	1/m
VG parameter, n	5.565	1.5	1.6	1
VG parameter, m	0.461	0.333	0.375	1
Saturated hydraulic conductivity, K_s	1.1×10^{-4}	7.0×10^{-6}	5.8×10^{-7}	m/s
Mass fraction of the clay, f_c	0.07	0.2	1	1
Empirical regression parameter, b_1	0.228	0.243	-0.197	W/m/K
Empirical regression parameter, b_2	-2.406	0.393	-0.932	W/m/K
Empirical regression parameter, b_3	4.909	1.534	2.521	W/m/K
Resource	Lu (2016)	Chung and Horton (1987)	Wang and Huang (2010)	/

3 NUMERICAL SIMULATION RESULTS AND DISCUSSION

In this section, we simulate the hydrothermal coupled process in three types of soils. The effects of soil types and initial water content on the water distribution are discussed and we analyze whether water or vapor played a major role in the migration process under different circumstances.

3.1 Numerical simulation of different soil types

Figure 2 shows the water and temperature distributions of three types of soils with a constant lower boundary effective saturation (40%) at different times. The initial distribution of water content indicates that the clay has the greatest capacity to retain water since the effective saturation of the whole soil column is close to that of the boundary while that of the sand surface is nearly zero. After applying a low temperature (278.15 K) to the upper surface, it can be seen that the temperature in the soil column rapidly declined during the first 5 d, and the absolute value of the temperature gradient becomes larger as the position approached the cold end of the soil column as shown in Figures 2b, 2d, and 2f. With increasing times, the temperature reaches an equilibrium and remains constant throughout the whole medium. Moreover, due to the different thermal conductivity intensities, the equilibrium is reached respectively faster for the sand, loam and clay.

The water content of the top layer in three soils all increases after 90 d and already after 5 days, one can notice an increase of water content. Notwithstanding, the increase is not obvious in the sand as Figure 2a shows. So, to further comprehend this phenomenon, Figure 3 presents the volumetric flux of water and vapor, which is helpful to evaluate the role of water and vapor in the hydrothermal coupled migration process as well. One can see an inflection point at early stage (e.g., 5d) induced by the large water-vapor migration caused by the temperature gradient in the upper soil column (Figure 2) where q_l and q_{ve} are greatly high shown in Figure 3. Additionally, it is apparent from Figure 3 that vapor migration is most significant in the sand, followed by loam, and finally clay. On the one hand, the water content in the sand is extremely low, so the hydraulic conductivity of water (K_{lh} and K_{lT}) is small; on the other hand, the water retention capacity of the sand is relatively poorer compared to loam and clay according to Figure 1b. Therefore, we can conclude that the slight increase of water content at the top layer of the sand is due to the vapor migration. However, in the loam and clay, the increase is mostly owing to the water migration, especially in clay, because the volumetric flux of water is higher than that of vapor from Figures 3b and 3c. Due to the stronger water retention of the clay, downward water flow under gravity is relatively slow. Therefore, at 90 d, there is still an inflection point in the water distribution line of the clay, while it has disappeared in that of the loam.

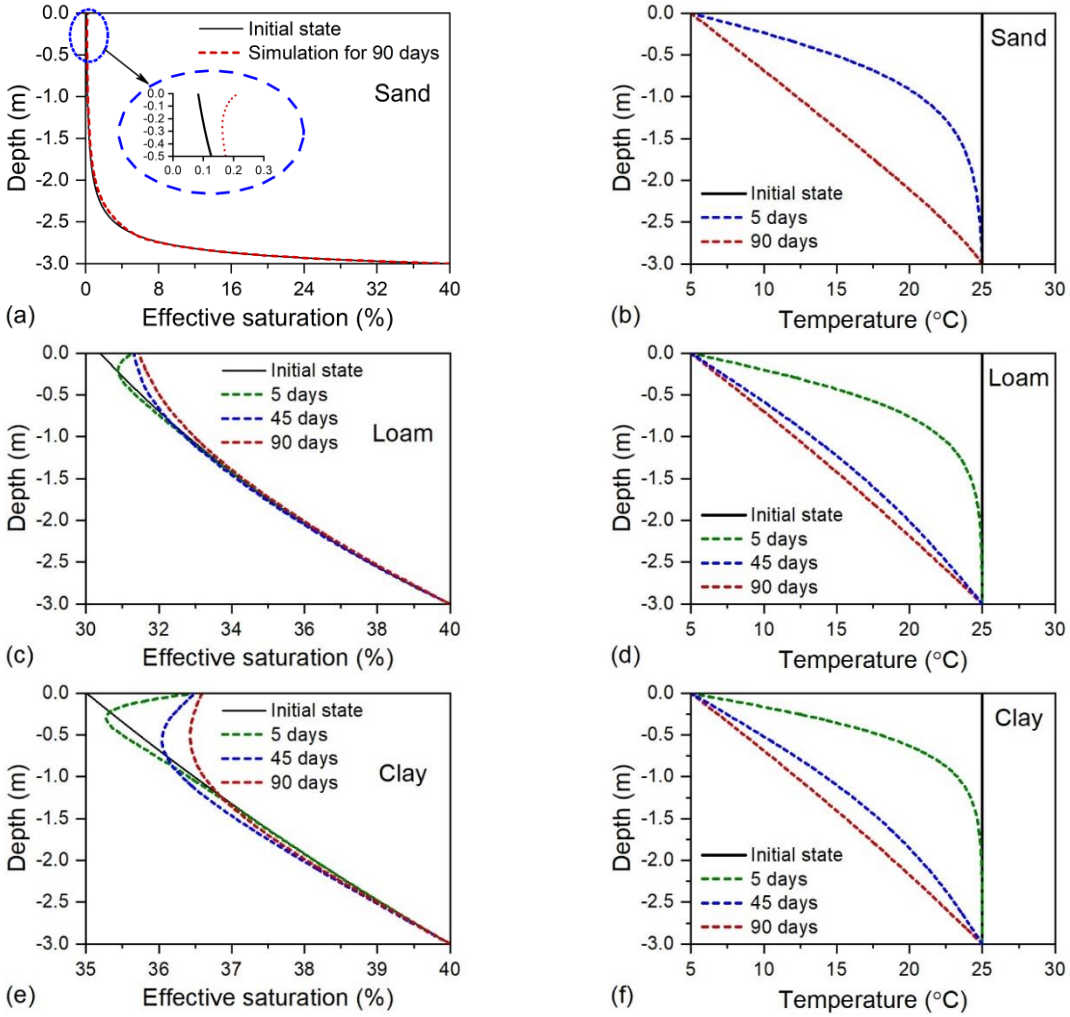


Figure 2. *Simulation results of water and temperature distributions of (a~b) sand, (c~d) loam, and (e~f) clay.*

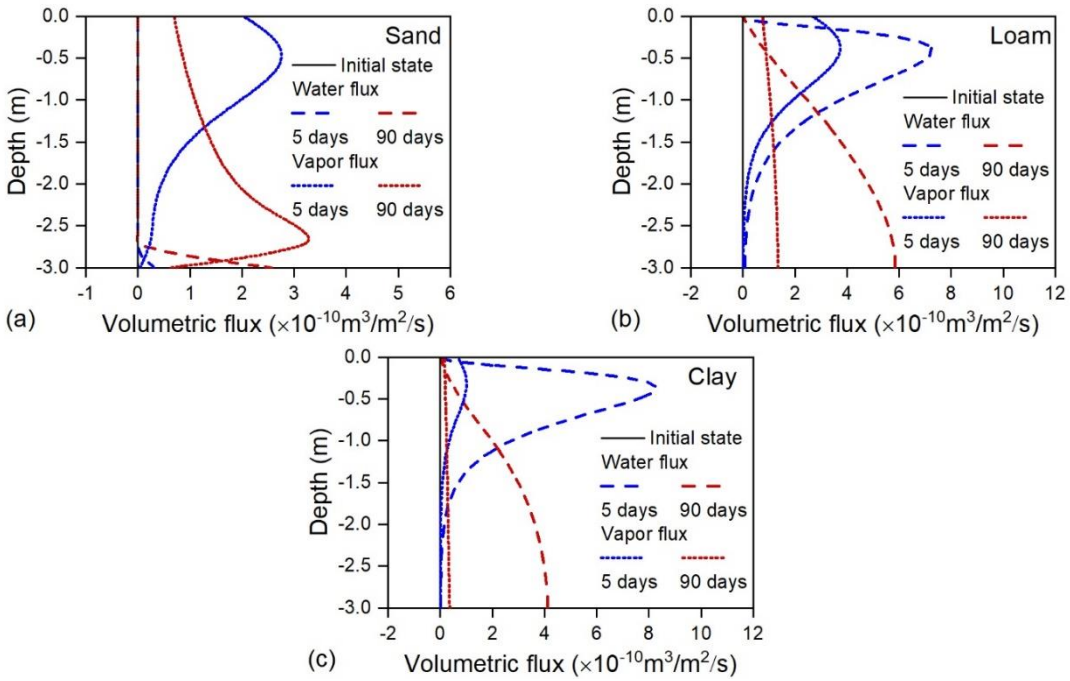


Figure 3. *Simulation results of water and vapor volumetric flux of different soil types. (a) Sand. (b) Loam. (c) Clay.*

3.2 Numerical simulation of different initial water contents

Since the change in water distribution in the sand is not obvious, we focus on the loam and clay to further analysis. Because the moisture content affects the hydraulic and thermal conductivities of soil and further influences the hydrothermal coupled process, it is essential to analyze the water-vapor migration under different initial water content. Figure 4 provides the water distributions at different times in the loam and clay with lower boundary saturation of 99%, which is nearly saturated. Compared to Figures 2c and 2e, the soil columns retain more water at the initial state, resulting in higher hydraulic conductivity and thermal conductivity of the soil. Thus, more water migrates to the cold end of the soil column under the hydraulic and temperature gradients, causing the increase of water content at the top layer. It can be seen from Figure 4 that the effective saturations of upper boundary increase approximately 3% and 4% in the loam and clay, respectively, which is higher than 1% and 1.5% in Figures 2c and 2e. The rate of reaching temperature equilibrium in the soil column is also faster due to the higher thermal conductivity of the soil.

Besides, θ_{ve} decreases accordingly since there is more water in the soil. The effect of vapor migration is further weakened and water migration dominates. Consequently, the water content near the surface of the soil column does not increase significantly in Figure 4 compared with Figures 2c and 2e (i.e., an inflection point is less noticeable). The volumetric vapor flux also decreases. Therefore, it can be assumed that the vapor migration is more dominant and cannot be ignored when the initial water content of the soil is extremely low.

The water distribution in the clay at 90 d is nearly linear as Figure 4 shows, and the water content at any depth is greater than the initial water content. It shows that the upward migration of water under the temperature gradient is greater than the downward migration under the hydraulic gradient in general. While in Figure 2c, both the temperature and hydraulic gradient cause the upward migration of water and vapor below the depth of about 1.2 m. This difference further indicates that water is more likely to evaporate and migrate upward to condense at a lower initial water content. When the initial water content is high, the upward migration of water also needs to be paid attention to.

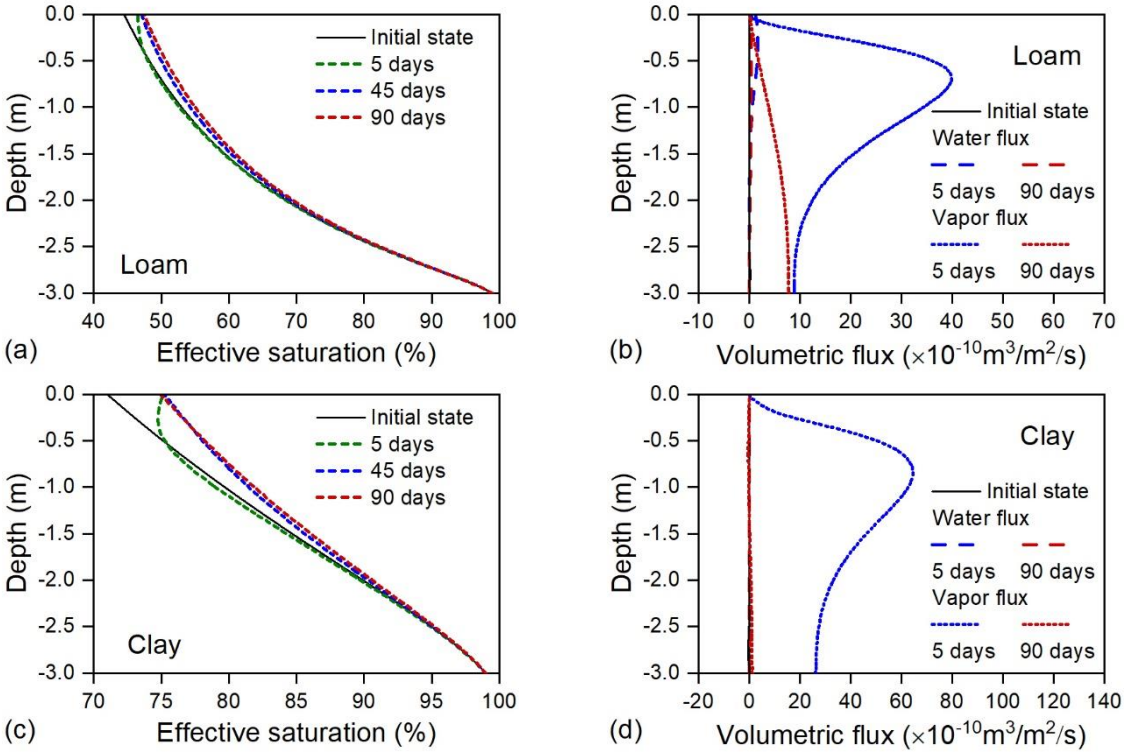


Figure 4. *Water distributions at different times in the loam and clay with effective saturation of 99% of the lower boundary. (a) Loam. (b) Clay.*

4 CONCLUSIONS

This study derives the governing equations of water-vapor and heat transfer in the framework of mass and energy conservation. A FEM model is established based on the derived equations to simulate the hydrothermal coupled migration process in different soil types, and the effect of initial water content is discussed. The main conclusions are summarized as follows.

The water content at the cold end of the soil columns increases according to the joint migration of water and vapor from the warm end to the cold end. The analysis of the volumetric flux of water and vapor demonstrates that vapor migration is more dominant in the sand than in loam and clay under the same temperature gradient. However, the increase in the water content in the sand is not noticeable due to the poor water retention capacity of sand. The increase in water content caused by the upward water migration under the temperature gradient in the loam and clay is significant and needs to be considered adequately. By comparing the simulation results of different initial water content, we conclude that the drier the soil, the more prominent the vapor migration.

Fully understanding the hydrothermal coupled migration in different soil layers is essential for solving engineering problems such as pavement cracking and frost heave. In this study, we gave a detailed analysis and found that both the water retention capacity of the soil and the initial water content should be taken into account in the analysis of the hydrothermal coupled migration, in which both water and vapor play important roles.

5 ACKNOWLEDGEMENTS

This research is supported by the National Natural Science Foundation of China (51979144) and the National Key Research and Development Program of China (2020YFC1806502).

REFERENCES

Chung, S.-O., & Horton, R. (1987). Soil heat and water flow with a partial surface mulch. Water resources research., 23(12), 2175-2186.

Côté, J., & Konrad, J.-M. (2005). A generalized thermal conductivity model for soils and construction materials. Canadian Geotechnical Journal, 42(2), 443-458.

De Vries, D. A. (1958). Simultaneous transfer of heat and moisture in porous media. Transactions - American Geophysical Union, 39(5), 909-916.

Li, Z. M., Chen, J., Tang, A. P., & Sugimoto, M. (2021). A novel model of heat-water-air-stress coupling in unsaturated frozen soil. International Journal of Heat and Mass Transfer, 175.

Lu, N. (2016). Generalized Soil Water Retention Equation for Adsorption and Capillarity. Journal of Geotechnical and Geoenvironmental Engineering, 142(10).

Orakoglu Firat, M. E. (2021). Experimental study and modelling of the thermal conductivity of frozen sandy soil at different water contents. Measurement, 181.

Philip, J. R., & De Vries, D. A. (1957). Moisture movement in porous materials under temperature gradients. Transactions, American Geophysical Union, 38(2).

Saito, H., Šimůnek, J., & Mohanty, B. P. (2006). Numerical Analysis of Coupled Water, Vapor, and Heat Transport in the Vadose Zone. Vadose Zone Journal, 5(2), 784-800.

Smits, K. M., Cihan, A., Sakaki, T., & Illangasekare, T. H. (2011). Evaporation from soils under thermal boundary conditions: Experimental and modeling investigation to compare equilibrium- and nonequilibrium-based approaches. Water Resources Research, 47(5).

Song, E. X., Luo, S., Kong, Y. F., & Li, P. (2017). Simulation and analysis of pot-cover effect on moisture transport in subgrade soil. Yantu Lixue/Rock and Soil Mechanics, 38(6), 1781-1788.

van Genuchten, M. T. (1980). A Closed-form Equation for Predicting the Hydraulic Conductivity of Unsaturated Soils. Soil Science Society of America Journal, 44(5), 892-898.

Wang, J., & Huang, S. (2010). Effect of soil water characteristic models on numerical modeling of unsaturated flow. Chinese Journal of Hydrodynamics, 25(1), 16-22.

Zhang, S., Teng, J., He, Z., Liu, Y., Liang, S., Yao, Y., & Sheng, D. (2016). Canopy effect caused by vapour transfer in covered freezing soils. Géotechnique, 66(11), 927-940.